Structural and electronic properties of SnS_2 stacked nanosheets: An *ab-initio* study

H. B. Mabiala-Poaty[a,b], D. H. Douma[a,b], B. M'Passi-Mabiala[a,b], R. E. Mapasha[c]

[a] *Groupe de Simulations Numériques en Magnétisme et Catalyse (GSMC), Facult des Sciences et Techniques, Université Marien Ngouabi, BP 69 Brazzaville-Congo, Congo.*
[b] *Unité de Recherche en Nanomatériaux et Nanotechnologies, Institut National de Recherche en Sciences Exactes et Naturelles (IRSEN), Brazzaville,Congo.*
[c] *Department of Physics, University of Pretoria, Pretoria 0002,South Africa.*

Abstract

We present an *ab-initio* study of the structural and electronic properties of SnS_2 stacked nanosheets using the standard LDA and GGA functionals as well as the newly developed variants of the non-local van der Waals (vdW) exchange correlation functionals, namely vdW-DF-revPBE and vdW-DF2-C09. We have examined different stacking configurations of the two, three and four SnS_2 layers. The GGA-PBE functional fails to describe the interlayer binding energies and interlayer spacing of SnS_2 nanosheets, while a good agreement is observed between the calculated and available experimental values when the van der Waals corrected functionals are used, mostly the vdW-DF2-C09. It is found that the interlayer interactions in the SnS_2 films are not only vdW type but, the overlap of wave functions of neighboring layers have to be taken into account. We have observed a systematic reduction in the band gap with the increase in the number of stacked layers. This can be another way of controlling the band gap of SnS_2 nanosheets as required for electronic devices.

Keywords: DFT, nanosheets, van der Waals exchange correlation functionals, electronic structure, 2D materials, SnS_2.

1. Introduction

After the successful synthesis of freestanding graphene [1, 2], the interest in graphene-like materials such as MoS_2, WS_2, SnS_2 etc [3] gained a lot of attention. Owing to their exotic properties such as transparency, high charge carrier mobility, flexibility etc [4, 5, 6], these type of materials stand a chance to be integrated into electronic and optoelectronic devices [7, 8]. However, in some instances, the relatively large band gap in some of these two dimensional (2D) materials limits their direct integration in the nanotechnological devices. It has been proven for MoS_2 nanosheets [9] that doping and various stacking sequences can be the possible ways of altering its properties to meet the technological application requirements.

The response of the electronic structure of SnS_2 nanosheets on the doping and change in stacking sequence deserves to be investigated. Recently, Joshi *et al.* [7] have successfully synthesized few SnS_2 nanosheets stacked layers using photosensitive field emission for optoelectronic application. They found that the band structure can explain the enhanced field emission current along with photoswitching property when SnS_2 nanosheets are illuminated by visible light source.

Bacaksiz *et al.* [10] have investigated the electronic properties of SnS_2 bilayer based on the *ab-initio* calculations. They reported that the interaction between layers is weaker in a SnS_2 bilayer than that of MoS_2 bilayer. Interestingly, the electronic properties of the SnS_2 bilayer depend on the type of stacking sequence[10]. Kumar *et al.* [11] also demonstrated that few layers stacking sequences fine tune the band gap of the MoS_2, WS_2, $MoSe_2$, WSe_2, $MoTe_2$ and WTe_2. They reported that the electronic structure of AA-stacked and AB-stacked sequences seems to be the same. The only difference is that AA-stacked has a higher band gap (1.31 eV) compared to AB-stacked (1.21 eV) sequence.

The stacked layers are mainly coupled together by the weak van der Waals forces (vdW). The vdW forces are known to be the relatively soft and weak interactions caused by the correlations in the rapidly fluctuating polarization in

the two separated fragments such as atoms, molecules, etc [12]. The standard density functional theory (DFT) exchange correlation functionals (generalized gradient approximation (GGA) and local density approximation (LDA)) are not formulated to capture these forces. This is due to the missing of one of the energy term which accounts for long range attraction in Kohn-Sham equations [13]. To improve the failure of GGA, several density functionals which take vdW forces into account have been theoretically developed [14]. Among them are the newly developed non-local vdW density functionals (vdW-DF) [15, 16, 17, 18, 19] which greatly depend on the electronic density. The first vdW-DF functional is the vdW-DF-revPBE which uses the semi-local exchange energy functional known as revised Perdew Buke Ernzerhof (revPBE) [20]. This functional generally predicts the relatively weak binding energy between the layers and it severely overestimates the interlayer spacing [21, 15]. To solve this overestimation and improve the binding energy, the vdW-DF2-C09 [21, 22, 23] has been used and proved to be suitable (C09 is the cooper exchange energy term).

Seminovski *et al.* have studied the structural and electronic properties of SnS_2 bilayer using the semi-empirical van der Waals corrected exchange-correlation functional [24] known as DFT-D2$_{Grimme}$[14]. They found its interlayer spacing to be closer to the experimental value but the band gap was underestimated. The band gap values were improved when DFT-D2$_{Grimme}$ is combined with the Heyd-Scuseria-Ernzerhof (HSE) functional. Short recently, Li *et al* [25] have just demonstrated that the thermoelectric performance of SnS_2 is enhanced by reducing its thickness from bulk to few layers stacked. Furthermore, the knowledge of dependence of the electronic structure on the stacking sequence configurations at each number of layers is still lacking.

In the present work, we study the stability, structural and electronic properties of SnS_2 stacked nanosheets using DFT methods. We consider a stacking of up to four layers and investigate all the possible stacking sequence configurations at each number of layers (AA, AB, AAA, AAB, AAAA, ABAB etc.). The behavior of these newly studied multilayer configurations suggests that this can be

a way of controlling the band gap of SnS_2 nanosheets to meet the requirements for electronic applications. We compare the results of standard LDA and GGA functionals with those of vdW-DF-revPBE, vdW-DF2-C09 and experimental results.

This paper is organized as follows: in section 2, we describe the computational details used in this study. In section 3, we investigate the structural and electronic properties of a single and stacked multilayers of SnS_2. The conclusion is given in section 4.

2. Methodology

First principle calculations have been performed with QUANTUM ESPRESSO code [26] using a plane wave basis set in pseudopotential approach and periodic boundary conditions. We use the well-known LDA and GGA functionals, and the newly developed variants of non-local van der Waals exchange correlation functionals, namely vdW-DFrevPBE and vdW-DF2-C09 which allow us to take account for the vdW forces [15, 22, 23]. The Kohn-Sham (KS) orbitals and the charge density are represented using basis sets consisting of PWs up to a maximal kinetic energy of 35 Ry and 350 Ry, respectively. The Brillouin zone is sampled using the Monkhorst-Pack scheme [27] with $7 \times 7 \times 1$ k-points mesh for GGA, vdW-DFrevPBE and vdW-DF2-C09 functionals, and $10 \times 10 \times 1$ k-points mesh for LDA. We have used the supercells consisting of 3, 6, 9 and 12 atoms for one, two, three and four layers respectively. The layers are separated from their periodic images by at least 15 Å in order to minimize their mutual interactions. The convergence parameters are 10^{-8} Ry on the total energy of self consistent cycle and 10^{-8} Ry/Bohr on the forces for the atomic relaxation. It is well known that LDA and GGA functionals underestimate the electronic band gap energy. In order to obtain more accurate band gap values, the GGA+U approach suggested by Dudarev *et al* [28] is used to cope with the strong correlation effect of the localised Sn-4d and S-3p states. Therefore, the Hubbard values of 9 eV and 3.8 eV are chosen for Sn-4d and S-3p electrons to reproduce

the experimental band gap of SnS_2.

3. Results and Discussion

Before considering the stacked multilayers of SnS_2, we investigate the electronic properties of the two phases of SnS_2 monolayer (1H-SnS_2 and 1T-SnS_2) as predicted by DFT methods. Indeed, the SnS_2 monolayer has two phases, namely, the 1H and 1T phases. The unit cell of both phases is a hexagonal prism. They have a layered structure, with Sn atom sandwiched between two S atoms. The main difference between the crystal structures of the two phases is found in the way of sandwiching the Sn atoms. The 1H phase is the trigonal prismatic type, i.e, the S layers occupy the equivalent positions (see Fig.1(a)). Its space group is $p\overline{6}m2$. In the 1T phase, the S layers are closed packed (see Fig.1(b)). The 1T phase is the antiprismatic (or octahedral) type and belongs to the $p\overline{3}m2$ space group.

We used only the GGA functional to optimize the two phases, since there is no interlayer interaction involved. The obtained equilibrium lattice parameters and nearest neighbor bondlengths (Sn-S) for 1H and 1T phases are presented in Table 1 and compared with available literature. The calculated a_0 of 3.62 Å and 3.70 Å obtained respectively for 1H and 1T phases are in good agreement with the experimental values of 3.65 Å [29], and theoretical GGA one of 3.60 Å for 1H [30] and 3.69 Å for the 1T phase [30]. We found the uniform nearest neighbor S-Sn of 2.64 Å and 2.60 Å for 1H and 1T phases respectively (see Table 1). The 1H-SnS_2 is higher 851 meV in energy with respect to the 1T-SnS_2. This confirm that the formation of 1T phase is more favorable than 1H one. These results are in agreement with the previous works (see Table 1). The slight overestimation of GGA functional on the description of covalently bonded structures is known for different class of materials. Fig.2 shows the band structures of both SnS_2 phases. In agreement with the previous studies [10, 30], the two phases are the indirect semiconducting compound. The valence band maximum (VBM) of 1H-SnS2 is located at the Γ-high symmetry point while the conduction band

minimum (CBM) is seen at the M-point (see Fig.2(a)). In the case of the 1T-SnS_2, the VBM is between Γ and M points and the CBM at the M-point (see Fig.2(b)). The calculated Partial and Total Density of States (TDOS and PDOS) show in Figs.2(c) and 2(d) that, the VBM of 1H-SnS_2 and 1T-SnS_2 is dominated by p states of S atoms, while their CBM are mainly formed by the hybridization of s states of Sn atoms and p states of S atoms.

As given in Table 1, the band gaps of 0.75 eV and 1.57 eV are found for 1H-SnS_2 and 1T-SnS_2 respectively. These obtained band gap values are closer to the available theoretical results: 0.78 eV and 1.57 eV for 1H and 1T phases respectively [30]. As confirmed by our results, the 1T is the most energically favorable phase of SnS_2 monolayer, then we perfom all the calculations on the stackings with the 1T phase.

The structural and electronic properties of 1T-SnS_2 monolayer are also calculated using LDA functional before starting the stackings. The optimized structural parameters are given in Table 2 and agree with the previous experimental and theoretical available values.

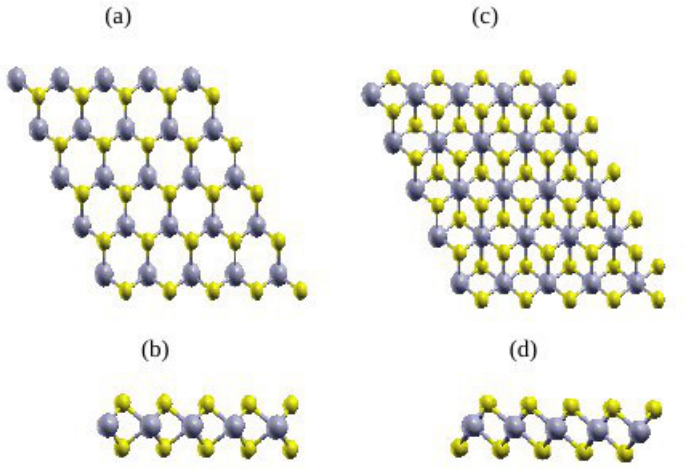

Fig. 1 (a) and (b) top view and side view respectively of 1H-SnS_2. (c) and (d) top view and side view respectively of 1T-SnS_2 monolayer. Each sulfur atom (yellow ball) has three neighbors tin atoms (grey ball).

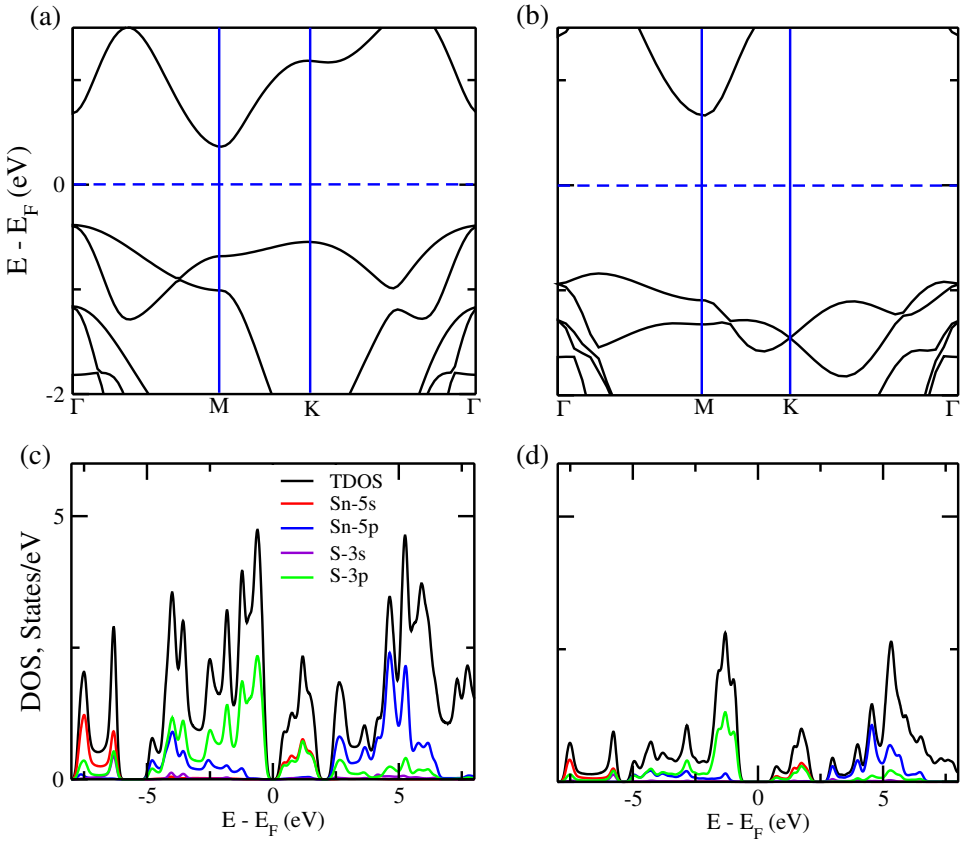

Fig. 2 (color online) (a) and (b) represent the calculated band structures of 1H and 1T SnS_2, respectively. (c) and (d) are the total and partial DOS of 1H and 1T SnS_2. These curves are obtained using GGA-PBE functional, The Fermi energy is set to zero.

Table 1: The calculated equilibrium lattice parameter a_0, tin-sulfure bondlenght b_{Sn-S}, band gap E_g and energy differences calculated between 1T-SnS_2 and 1H-SnS_2.

SnS_2	a_0(Å)	b_{Sn-S}(Å)	E_g(eV)	ΔE(eV)
1T	3.70	2.60	1.57	0.00
1H	3.62	2.64	0.75	0.85
1T-[30]	3.69	2.59	1.58	0.00
1H-[30]	3.60	2.63	0.78	0.87

In the next discussion, we have shown that the GGA functional fails to correctly predict the equilibrium interlayer spacing (d_0) of different stackings of van der Waals forces bonded two, three and four SnS_2 monolayers, and we also tested the newly developed variants of non-local van der Waals exchange correlation functionals, namely vdW-DF-revPBE and vdW-DF2-C09. We started with the description of the possible stackings of two SnS_2 layers. The two SnS_2 layers can be stacked into two configurations with different orientations namely, the AA-stacking and the AB-stacking as shown in Figs.3 . In the AA-stacking, the Sn atoms are directly facing the Sn atoms on the adjacent layer. The S atoms face the covalent bonds between the S and Sn on the adjacent layer. In the AB-stacking, the S atoms face directly on top of S atoms on the adjacent layer. The Sn atoms face the covalent bonds between the S and Sn on the adjacent layer (see Fig.3).

Firstly, we have examined how the newly developed variants of non-local van der Waals exchange correlation functionals, namely vdW-DF-revPBE and vdW-DF2-C09 describe the in-plane bondlengths (a_0 and b_{Sn-S}) of the coupled AA-stacking, AB-stacking sequence configurations as compared to the standard functionals and experimental values. Table 2 shows that in all the configurations considered, the values of a_0 and b_{Sn-S} obtained using vdW-DF-revPBE are slightly larger than those predicted by vdW-DF2-C09, GGA and LDA functionals. For instance, a lattice parameter of 3.78 Å is obtained for AA-stacking

using vdW-DF-revPBE, whereas it is 3.67 Å for vdW-DF2-C09, 3.64 Å for LDA and 3.71 Å for GGA-PBE. The vdW-DF2-C09 and LDA exchange correlation functionals predict a_0 of much closer to an experimental value of 3.65 Å[29]. On the other hand, the bondlengths of 2.64 Å (vdW-DF-revPBE), 2.58 Å (vdW-DF2-C09), 2.56 Å (LDA) and 2.60 Å (GGA-PBE) are noted in Table 2 for AA stacking sequence configuration. Generally, all the exchange correlation functionals agree well with the predicted in-plane bond distances[31].

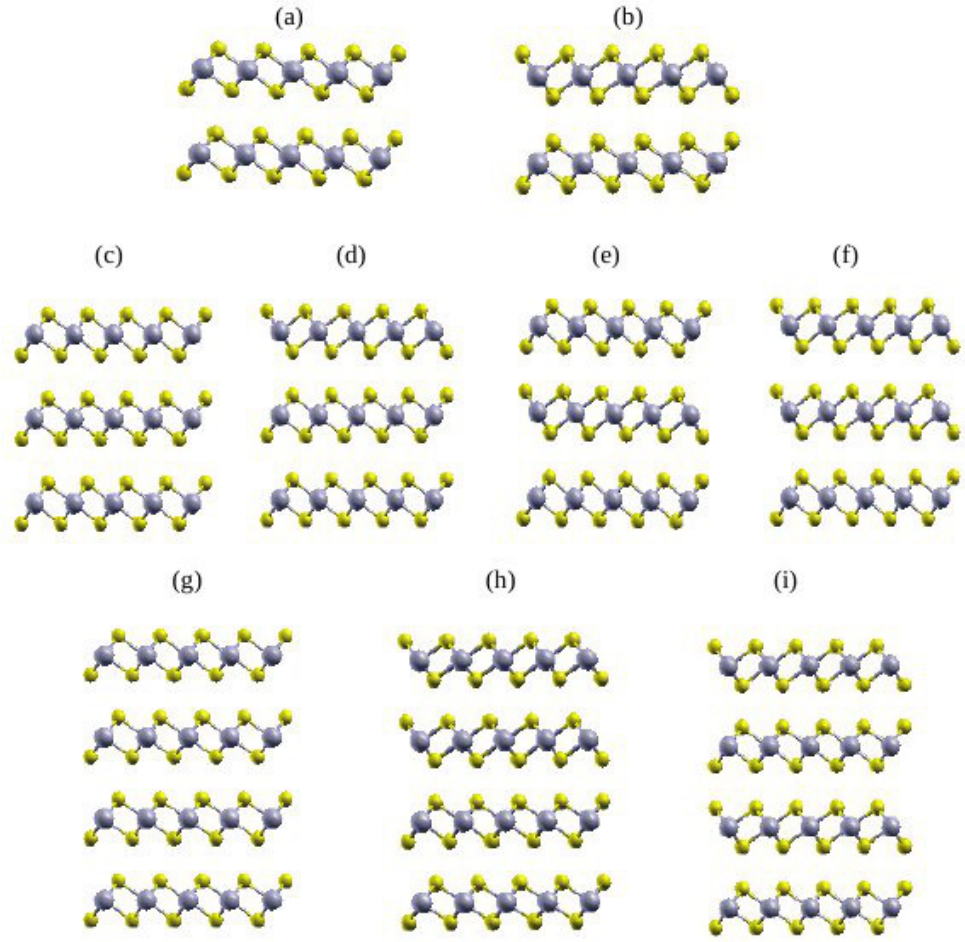

Fig. 3 (Color online) Crystal structure of SnS_2 stacked layers (a) AA, (b) AB, (c) AAA, (d) AAB, (e) ABA, (f) ABB, (g) AAAA, (h) AABB and (i) ABAB.

Table 2: Dependence of the physical properties of bulk and SnS_2 layers on the stacking sequences and different exchange correlation functionals. a_0 is the lattice parameter, b_{Sn-S} is the bondlength between the nearest neighbor Sn and S atoms, d_0 and c are the interlayer spacing, while E_b and E_g are the binding energy and band-gap respectively. d_0 has several values separated by slash in the case of three and four stacked layers. The character (*) means the value is not available. The values of band gap in parentheses are obtained using the GGA+U method.

Stacked layer	Parameters	GGA	LDA	vdW-DFrevPBE	vdW-DF2-C09	Experiment	Theory
	a_0(Å)	3.70	3.63	*	*	3.65[29]	3.70[24]
Single	b_{Sn-S}(Å)	2.60	2.56	*	*	2.60[32]	2.59[32]
layer	E_g(eV)	1.57(2.20)	1.44	*	*	2.23[29]	1.57[33]
	a_0(Å)	3.64	3.65	3.76	3.69	3.64[34]	3.70[35]
Bulk	b_{Sn-S}(Å)	2.60	2.57	2.63	2.59	2.59[32]	2.57[36]
	c(Å)	5.99	5.89	6.07	5.95	5.88[34]	6.88[35]
	E_g(eV)	1.52(2.12)	1.30	1.40(2.17)	1.44(2.12)	2.18[35]	2.18 [37]
	a_0(Å)	3.71	3.64	3.78	3.67	*	*
	b_{Sn-S}(Å)	2.60	2.56	2.64	2.58	*	
AA	d_0(Å)	6.82	5.61	6.31	5.82	5.86 [24]	
	E_b(eV/cell)	-0.009	-0.137	-0.189	-0.183		
	E_g(eV)	1.51(2.14)	1.30	1.44(2.05)	1.37(2.03)	*	1.50 [24]
	a_0(Å)	3.71	3.62	3.71	4.03	*	*
	b_{Sn-S}(Å)	2.65	2.62	2.69	2.64	*	*
AB	d_0(Å)	7.47	6.65	6.88	6.93	*	*
	E_b(eV/cell)	-0.019	-0.051	-0.145	-0.151	*	*
	E_g(eV)	1.48(2.11)	1.33	1.43(1.98)	1.35(1.96)	*	*

We further examined how the newly developed variants of non-local van der Waals exchange correlation functionals and standard functionals describe the interlayer interaction by calculating d_0 and interlayer binding energy (E_b) of coupled AA-stacking and AB-stacking sequence configurations. To examine the energetic stability of each stacked configuration, the interlayer binding energies (E_b) defined below was considered:

$$E_\mathrm{b} = E_\mathrm{layers} - nE_\mathrm{layer}, \tag{1}$$

in which E_layers, n and E_layer are the energy of the stacked layers, the number of layers and the energy of a single layer respectively. According to Eq.(1), a negative value of E_b corresponds to a stable coupled configuration while a positive value corresponds to an unstable uncoupled configuration. All the E_b results presented in Table.2 are found to be negative for the two stacking configurations (AA and AB stackings) from all the exchange-correlation functionals employed revealing that the SnS_2 layers prefer to be coupled together. Results show that the AA-stacking gives a more stable bilayer structure than the AB-stacking. The AB-stacking gives the binding energy, which is 0.08 eV/Cell (LDA), 0.04 eV/Cell (vdW-DF-revPBE), and 0.03 eV/Cell (vdW-DF2-C09) lower than in the corresponding binding energy in the AA-stacking. The calculated interlayer binding energies in the present work are whithin the range of experimental and theoretical values, where the results are presented in meV/Å^2 [38, 39].

We have also calculated the d_0 of both AA and AB stackings, using all the functionals. The values of d_0 are shown in Table 2, and it turns out that the AB-stacking has the d_0 slightly larger than the AA-stacking. As expected, the magnitude of d_0 is strongly dependent on the exchange-correlation functional used. For both stackings, the GGA functional overestimates the interlayer spacing whereas the LDA predicts the values closer to the experiment. This is a clear indication of the failure of GGA functional to accurately describe the van der Waals bonded materials, and therefore requires non local vdW corrections. The non local vdW corrections is clearly useful for the cancellation of the errors ob-

served in the pure GGA functional, which could explained with the fact that the calculated d_0 using the vdW-DF2-C09 functional is closer to the experimental value [24]. We also observed that the LDA functional provide better evaluation of the interlayer spacing in the layered systems than the GGA functional. This property of LDA has been usually attributed to a fortunate cancellation of errors in the exchange-correlation functional [40, 31, 41]. The interlayer binding energies and interlayer spacing calculated with LDA and vdW-DF2-C09 functionals are found to be in the same magnitude order. The fact that the LDA functional provides the binding energies and the interlayer spacing close to the experimental values, suggest that the interlayer interactions in the SnS_2 films are not only vdW type but, the overlap of wave functions of neighboring layers have to be taken into account [41].

The configurations consisting of three (AAA, ABA, AAB and ABB) and four (AAAA, AABB and ABAB) stacked layers (see Fig.3) were examined (Table 3) and compared with the SnS_2 bulk results in Table 2. It turned out that the bulk interlayer distance c is in agreement with the stacked layers, for all the functionals used (see Tables 2 and 3).

We also examined the effects of the stacking sequences and the number of layers on the electronic properties of SnS_2, namely AA, AB, AAA, AAB, ABB, ABA, AAAA and ABAB stacked layers. The band structures presented in the case of AA and AAA (see Fig.4) are representative for all the configurations, since they are quite similar for the same number of layers despite the stacking sequence. The main difference between the band structures is the additional states at the vicinity of the Fermi level when adding one, two and three layers on the SnS_2 monolayer. As stated in the methodology section, to accurately describe the band gap, we have used the GGA+U method. It is clearly noted that the SnS_2 stacked coupled layers are indirect band gap semiconductors, regardless of stacking sequence. The band structures presented in Fig.4 show that the pure DFT calculations present the band gaps smaller than those obtained using GGA+U method. We apply the GGA+U just for a selected configurations (Single layer, AA, AAA, AAB, and ABAB stackings). Regardless the

Table 3: Dependence of the physical properties of bulk and SnS_2 layers on the stacking sequences and different exchange correlation functionals. a_0 is the lattice parameter, b_{Sn-S} is the bondlength between the nearest neighbor Sn and S atoms, d_0 and c are the interlayer spacing, while E_b and E_g are the binding energy and band-gap respectively. d_0 has several values separated by slash in the case of three and four stacked layers. The values of band gap in parentheses are obtained using the GGA+U method.

Stacked-layers	Parameters	GGA	LDA	vdW-DFrevPBE	vdW-DF2-C09
	a_0(Å)	3.71	3.64	3.78	3.67
	b_{Sn-S}(Å)	2.60	2.56	2.65	2.58
AAA	d_0(Å)	6.80/6.87	5.62/5.53	6.27/6.31	5.86/5.83
	E_b(eV/cell)	-0.016	-0.270	-0.377	-0.368
	E_g(eV)	1.51(2.13)	1.15	1.41(2.04)	1.36(1.93)
	a_0(Å)	3.71	3.63	3.78	3.65
	b_{Sn-S}(Å)	2.60	2.56	2.63	2.58
AAB	d_0(Å)	6.96/7.52	5.61/6.55	6.46/6.98	5.83/6.92
	E_b(eV/cell)	-0.014	-0.182	-0.328	-0.280
	E_g(eV)	1.50(2.13)	1.17	1.39(1.98)	1.35(1.82)
	a_0(Å)	3.69	3.62	3.78	3.65
	b_{Sn-S}(Å)	2.60	2.58	2.64	2.58
ABA	d_0(Å)	7.64/7.49	7.45/7.48	6.89/6.83	7.45/7.48
	E_b(eV/cell)	-0.011	-0.037	-0.280	-0.136
	E_g(eV)	1.41	1.38	1.30	1.31
	a_0(Å)	3.71	3.71	3.80	3.67
	b_{Sn-S}(Å)	2.60	2.56	2.66	2.58
AAAA	d_0(Å)	6.90/6.92/6.93	5.62/5.65/5.63	6.28/6.28/6.28	5.83/5.85/5.81
	E_b(eV/cell)	-0.025	-0.404	-0.562	-0.561
	E_g(eV)	1.50	0.96	1.35	1.27
	a_0(Å)	3.60	3.63	3.75	3.65
	b_{Sn-S}(Å)	2.60	2.57	2.63	2.59
AABB	d_0(Å)	7.34/6.93/7.00	6.52/5.79/5.62	7.06/6.85/6.77	5.83/6.64/5.91
	E_b(eV/cell)	-0.031	-0.249	-0.607	-0.490
	E_g(eV)	1.50	1.04	1.40	1.32
	a_0(Å)	3.70	3.61	3.77	3.65
	b_{Sn-S}(Å)	2.60	2.57	2.64	2.58
ABAB	d_0(Å)	6.80/7.52/7.41	6.79/6.65/6.60	6.79/6.65/6.64	6.80/6.62/6.69
	E_b(eV/cell)	-0.014	-0.120	-0.435	-0.297
	E_g(eV)	1.27(1.95)	1.26	1.27(1.92)	1.27(1.88)

configuration, the functional and method used, we observed that the VBM is located between Γ and M high symetry points, while the CBM is located at M point. Only the band structure calculated with LDA functional present the CBM between K and Γ points. All the results are reported in the Tables 2 and 3 and, one can see that the band gap decreases with the increase in the number of SnS_2 stacked layers. This observation is in agreement with Bacaksiz *et al* [10] for SnS_2 single and bilayers using the GGA functional as well as the semi-empirical Grimme correction (for the van der Waals interaction description) [14], and on the other hand by Gonzales *et al* [35] for two, three and four SnS_2 layers . The AA-stacking is identified as the one that maximize the band gap of SnS_2, whereas ABAB-stacking possesses the least. The band gap values of 1.51 eV (GGA), 1.30 eV (LDA), 1.44 eV (vdW-DF-revPBE) and 1.37 eV (vdW-DF2-C09) are found for this configuration. The same trend is observed with GGA+U method (see Tables 2 and 3). The vdW-DF2-C09 functional that accurately predict the structure and energetic, precisely reveals that the band gap of SnS_2 is not stacking sequence dependent as shown in Tables 2 and 3 (see band gaps of AA and AB also for AAA, AAB, ABA, ABB), but can be altered by the variation in number of layers.

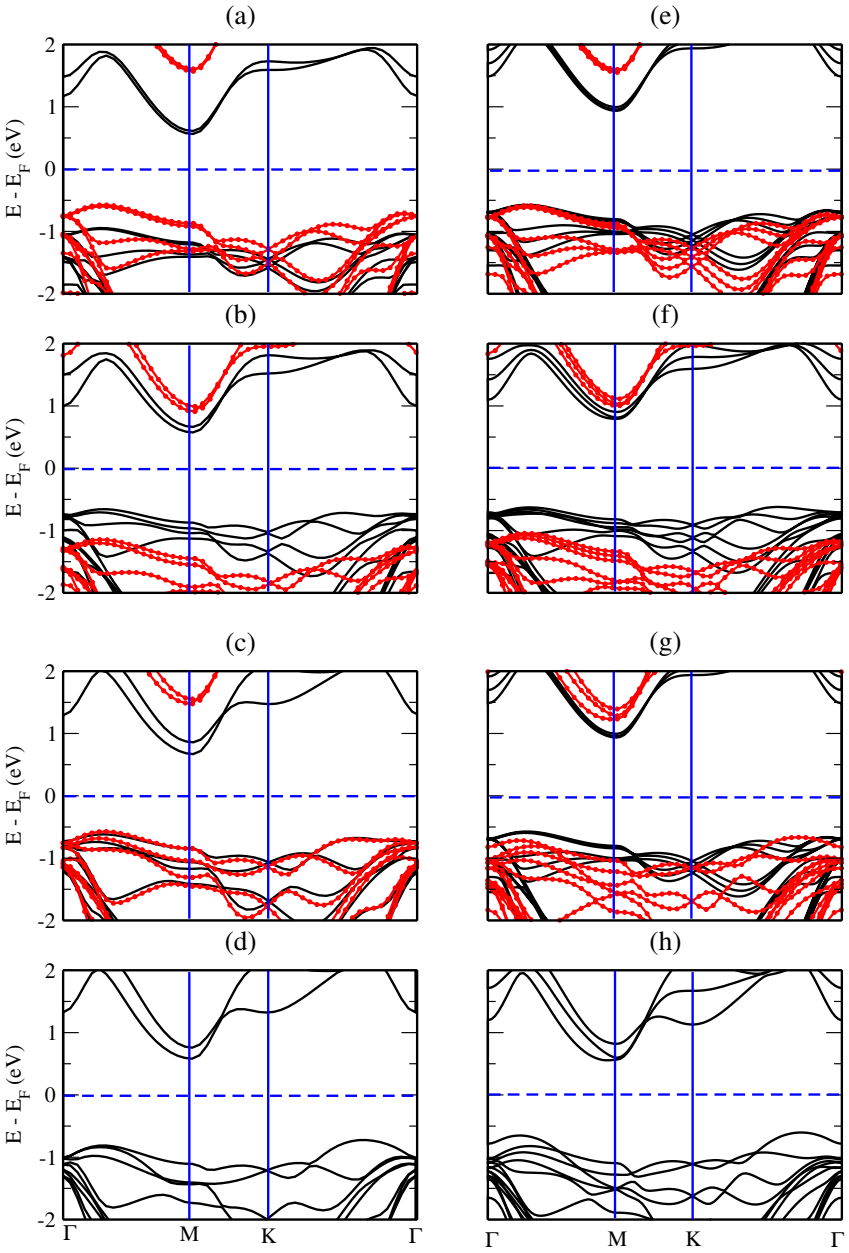

Fig. 4 (Color online) (a)-(d) band structures plots of SnS_2 AA stacking and (e)-(h) band structures of AAA stacking, calculated using GGA-PBE, vdW-DFrevPBE, vdW-DF2-C09 and LDA functionals respectively. The black curves and curves with red-circles are for pure DFT and DFT+U respectively.

4. Conclusion

We have investigated the energetic stability, structural and electronic properties of various stacking configurations of SnS_2 nanosheets using the standard LDA and GGA functionals, and the newly developed variants of non-local van der Waals exchange correlation functionals, namely vdW-DFrevPBE and vdW-DF2-C09 functionals. The GGA functional fails to accurately predict the interlayer binding energies and interlayer spacing of all the structures studied. The use of vdW corrections allowed the cancellation of errors observed in the semilocal functional (GGA), leading to a good agreement with experimental values. This trend is improved mostly when the cooper exchange energy (C09) is applied. Our results also show that the interlayer interactions in the SnS_2 films are not only vdW type but, the overlap of wave functions of neighboring layers have to be taken into account. All the van der Waals functionals underestimate the energy band gap of SnS_2 nanosheets, revealing that they were not formulated for improvement of the electronic properties description. All the functionals have shown that the AA, AAA and AAAA configurations are most energetically stable, have the shortest interlayer spacing and are semiconductors. The band gap of this stacking sequence decreases with the increase in the number of SnS_2 stacked layers. This reduction in the band gap is clearly described when applying GGA+U including vdW-DF2-C09 functional. The deviation of band gap with respect to stacking sequence and number of layers is necessary for controlling the electronic devices. In addition, the reduction of the band gap can be explored to develop several novel applications which includes energy storage, photonics, photocatalysis.

Acknowledgments

We acknowledge the computational resources provided by the Center for Hight Performance Computing (CHPC) in South Africa. Calculations in this work have been done using the plane-wave self-consistent field (PWscf) code [26],

distributed with the Quantum ESPRESSO package. The authors are grateful to B. R. Malonda-Boungou and N. F Andriambelaza for constructive suggestions.

References

References

[1] K. S. Novoselov, A. K. Geim, S. V. Morozov, D. Jiang, Y. Zhang, S. V. Dubonos, I. V. Grigorieva, A. A. Firsov, Electric field effect in atomically thin carbon films, science 306 (5696) (2004) 666–669.

[2] K. Novoselov, D. Jiang, F. Schedin, T. Booth, V. Khotkevich, S. Morozov, A. Geim, Two-dimensional atomic crystals, Proceedings of the National Academy of Sciences of the United States of America 102 (30) (2005) 10451–10453.

[3] R. Gordon, D. Yang, E. Crozier, D. Jiang, R. Frindt, Structures of exfoliated single layers of ws 2, mos 2, and mose 2 in aqueous suspension, Physical Review 65 (12) (2002) 125407.

[4] B. W. Baugher, H. O. Churchill, Y. Yang, P. Jarillo-Herrero, Intrinsic electronic transport properties of high-quality monolayer and bilayer mos2, Nano letters 13 (9) (2013) 4212–4216.

[5] H.-J. Chuang, X. Tan, N. J. Ghimire, M. M. Perera, B. Chamlagain, M. M.-C. Cheng, J. Yan, D. Mandrus, D. Tomnek, Z. Zhou, High mobility wse2 p-and n-type field-effect transistors contacted by highly doped graphene for low-resistance contacts, Nano letters 14 (6) (2014) 3594–3601.

[6] W. Liu, J. Kang, D. Sarkar, Y. Khatami, D. Jena, K. Banerjee, Role of metal contacts in designing high-performance monolayer n-type wse2 field effect transistors, Nano letters 13 (5) (2013) 1983–1990.

[7] Photosensitive field emission study of sns2 nanosheets, Journal of Vacuum Science & Technology B, Nanotechnology and Microelectronics: Materials, Processing, Measurement, and Phenomena 33 (3) 03C10.

[8] Y. Zhang, J. Ye, Y. Matsuhashi, Y. Iwasa, Ambipolar mos2 thin flake transistors, Nano letters 12 (3) (2012) 1136–1140.

[9] K. Dolui, I. Rungger, C. D. Pemmaraju, S. Sanvito, Possible doping strategies for mos 2 monolayers: An ab initio study, Physical Review B 88 (7) (2013) 075420.

[10] C. Bacaksiz, S. Cahangirov, A. Rubio, R. T. Senger, F. M. Peeters, H. Sahin, Bilayer sns 2: Tunable stacking sequence by charging and loading pressure, Physical Review B 93 (12) (2016) 125403.

[11] A. Kumar, P. Ahluwalia, Semiconductor to metal transition in bilayer transition metals dichalcogenides mx2 (m= mo, w; x= s, se, te), Modelling and Simulation in Materials Science and Engineering 21 (6) (2013) 065015.

[12] H. Hamaker, The londonvan der waals attraction between spherical particles, physica 4 (10) (1937) 1058–1072.

[13] J. P. Perdew, A. Zunger, Self-interaction correction to density-functional approximations for many-electron systems, Physical Review B 23 (10) (1981) 5048.

[14] S. Grimme, Semiempirical gga-type density functional constructed with a long-range dispersion correction, Journal of computational chemistry 27 (15) (2006) 1787–1799.

[15] M. Dion, H. Rydberg, D. C. Schröder, Elsebeth and, B. I. Lundqvist, Van der waals density functional for general geometries, Physical review letters 92 (24) (2004) 246401.

[16] H. Rydberg, B. I. Lundqvist, D. C. Langreth, M. Dion, Tractable nonlocal correlation density functionals for flat surfaces and slabs, Physical Review B 62 (11) (2000) 6997.

[17] H. Rydberg, M. Dion, N. Jacobson, E. Schröder, P. Hyldgaard, S. Simak, D. C. Langreth, B. I. Lundqvist, Van der waals density functional for layered structures, Physical review letters 91 (12) (2003) 126402.

[18] D. C. Langreth, M. Dion, H. Rydberg, E. Schröder, P. Hyldgaard, B. I. Lundqvist, Van der waals density functional theory with applications, International journal of quantum chemistry 101 (5) (2005) 599–610.

[19] D. C. Langreth, J. P. Perdew, Exchange-correlation energy of a metallic surface: Wave-vector analysis, Physical Review B 15 (6) (1977) 2884.

[20] Y. Zhang, W. Yang, Comment on generalized gradient approximation made simple, Physical Review Letters 80 (4) (1998) 890.

[21] R. E. Mapasha, A. M. Ukpong, N. Chetty, Ab initio studies of hydrogen adatoms on bilayer graphene, Physical Review B 85 (20) (2012) 205402.

[22] V. R. Cooper, Van der waals density functional: An appropriate exchange functional, Physical Review B 81 (16) (2010) 161104.

[23] K. Lee, É. D. Murray, L. Kong, B. I. Lundqvist, D. C. Langreth, Higher-accuracy van der waals density functional, Physical Review B 82 (8) (2010) 081101.

[24] Y. Seminovski, P. Palacios, P. Wahnón, Effect of van der waals interaction on the properties of sns2 layered semiconductor, Thin Solid Films 535 (2013) 387–389.

[25] J. Li, J. Shen, Z. Ma, K. Wu, Thickness-controlled electronic structure and thermoelectric performance of ultrathin sns2 nanosheets, Scientific Reports 7 (1) (2017) 8914.

[26] P. Giannozzi, S. Baroni, N. Bonini, M. Calandra, R. Car, C. Cavazzoni, D. Ceresoli, G. L. Chiarotti, M. Cococcioni, I. Dabo, et al., Quantum espresso: a modular and open-source software project for quantum simulations of materials, Journal of physics: Condensed matter 21 (39) (2009) 395502.

[27] H. J. Monkhorst, J. D. Pack, Special points for brillouin-zone integrations, Physical review B 13 (12) (1976) 5188.

[28] S. Dudarev, G. Botton, S. Savrasov, C. Humphreys, A. Sutton, Electron-energy-loss spectra and the structural stability of nickel oxide: An lsda+ u study, Physical Review B 57 (3) (1998) 1505.

[29] F. Al-Alamy, A. Balchin, M. White, The expansivities and the thermal degradation of some layer compounds, Journal of Materials Science 12 (10) (1977) 2037–2042.

[30] F. Raffone, C. Ataca, J. C. Grossman, G. Cicero, Mos2 enhanced t-phase stabilization and tunability through alloying, The journal of physical chemistry letters 7 (13) (2016) 2304–2309.

[31] O. Leenaerts, B. Partoens, F. Peeters, Hydrogenation of bilayer graphene and the formation of bilayer graphane from first principles, Physical Review B 80 (24) (2009) 245422.

[32] C. Xia, Y. Peng, H. Zhang, T. Wang, S. Wei, Y. Jia, The characteristics of n-and p-type dopants in sns 2 monolayer nanosheets, Physical Chemistry Chemical Physics 16 (36) (2014) 19674–19680.

[33] H. L. Zhuang, R. G. Hennig, Theoretical perspective of photocatalytic properties of single-layer sns2, Physical Review B 88 (11) (2013) 115314.

[34] M. Schlüter, M. L. Cohen, Valence-band density of states and chemical bonding for several non-transition-metal layer compounds: Snse2, pbi2, bii3, and gase, Physical Review B 14 (2) (1976) 424.

[35] J. M. Gonzalez, I. I. Oleynik, Layer-dependent properties of sns 2 and snse 2 two-dimensional materials, Physical Review B 94 (12) (2016) 125443.

[36] Y. Sun, H. Cheng, S. Gao, Z. Sun, Q. Liu, Q. Liu, F. Lei, T. Yao, J. He, S. Wei, et al., Freestanding tin disulfide single-layers realizing efficient visible-light water splitting, Angewandte Chemie International Edition 51 (35) (2012) 8727–8731.

[37] G. Domingo, R. Itoga, C. Kannewurf, Fundamental optical absorption in sn s 2 and sn se 2, Physical Review 143 (2) (1966) 536.

[38] T. Björkman, A. Gulans, A. V. Krasheninnikov, R. M. Nieminen, van der waals bonding in layered compounds from advanced density-functional first-principles calculations, Physical review letters 108 (23) (2012) 235502.

[39] F. A. Rasmussen, K. S. Thygesen, Computational 2d materials database: electronic structure of transition-metal dichalcogenides and oxides, The Journal of Physical Chemistry C 119 (23) (2015) 13169–13183.

[40] L. A. Girifalco, M. Hodak, Van der waals binding energies in graphitic structures, Physical Review B 65 (12) (2002) 125404.

[41] I. N. Yakovkin, Dirac cones in graphene, interlayer interaction in layered materials, and the band gap in mos2, Crystals 6 (11) (2016) 143.